Low-energy spin fluctuations in filled skutterudites $YbFe_4Sb_{12}$ and $LaFe_4Sb_{12}$ investigated through $^{121}Sb$ nuclear quadrupole and $^{139}La$ nuclear magnetic resonance measurements



2008 J. Phys.: Condens. Matter 20 195214

(http://iopscience.iop.org/0953-8984/20/19/195214)

J. Phys.: Condens. Matter **20** (2008) 195214 (8pp) doi:10.1088/0953-8984/20/19/195214

# Low-energy spin fluctuations in filled skutterudites $YbFe_4Sb_{12}$ and $LaFe_4Sb_{12}$ investigated through $^{121}Sb$ nuclear quadrupole and $^{139}La$ nuclear magnetic resonance measurements

**A Yamamoto[1,4], S Iemura[1], S Wada[1], K Ishida[2], I Shirotani[3] and C Sekine[3]**

[1] Department of Physics, Graduate School of Science, Kobe University, Kobe 657-8501, Japan
[2] Department of Physics, Graduate School of Science, Kyoto University, Kyoto 606-8502, Japan
[3] Faculty of Engineering, Muroran Institute of Technology, Mizumoto, Muroran 050-8585, Japan

Received 28 January 2008, in final form 17 March 2008
Published 11 April 2008
Online at stacks.iop.org/JPhysCM/20/195214

**Abstract**

We have elucidated low-energy spin fluctuations in the new filled skutterudites $YbFe_4Sb_{12}$ and $LaFe_4Sb_{12}$ synthesized at high pressures, through $^{121}Sb$ nuclear quadrupole resonance (NQR) and $^{139}La$ nuclear magnetic resonance (NMR) measurements. The longitudinal spin–lattice relaxation rate $1/T_1$ of $^{121}Sb$ in $YbFe_4Sb_{12}$ provides evidence that upon cooling below ~20 K, the compound transforms from the localized 4f electron state of $Yb^{3+}$ ions to a nonmagnetic heavy Fermi liquid state, originating from the mixing of 4f electrons with conduction electrons. Whereas, the Curie–Weiss type behaviour of the $^{139}La$ Knight shift and $^{121}Sb$-$1/T_1$ in $LaFe_4Sb_{12}$ indicate that the compound remains in the localized electron state down to 1.4 K, it in fact originates from 3d electrons of Fe in $[Fe_4Sb_{12}]$ anions. In both compounds, the transversal nuclear spin–spin relaxation rate $1/T_2$ exhibits a clear peak at $T^* \simeq 32$ and $\simeq$23 K, respectively. The origin of the $1/T_2$ peak is discussed in terms of the freezing of the thermal vibration of Sb cages or rare-earth ions filled in each Sb cage. By comparing the experimental results of the present study with those previously reported for the compounds synthesized at ambient pressure, it is pointed out that both the strongly correlated electron properties and the thermal vibrations are greatly modified with the increase of rare-earth atom deficiency.

## 1. Introduction

Recently, intensive experimental and theoretical investigations have concentrated on the rich phenomena shown by the filled skutterudites $RT_4X_{12}$ (R = rare-earth atom, T = transition-metal atom, X = pnictogen atom) such as the heavy fermion superconductivity, metal–insulator transition, and multipolar ordering [1]. The skutterudites have the bcc structure (space group; $Im\bar{3}$) where R can be filled as a guest in each cage formed by twelve ligand X atoms, and a consensus has been developed that this peculiar crystal structure allows 4f electrons of R ions to move by mixing with neighbouring p electron orbits, giving rise to the wide variety of strongly correlated electron phenomena. The heavy fermion state of the filled skutterudites is generally considered to be caused by a large extent of mixing $J_{cf}$ between the 4f electron and conduction electrons. However, the specific heat and transport measurements on the heavy Fermi liquid (HFL) skutterudite $SmOs_4Sb_{12}$ revealed that both the electronic specific heat coefficient $\gamma$ and the coefficient $A$ of the quadratic temperature-dependent term of the electrical resistivity do not show a

[4] Present address: Department of Physics, Graduate School of Science, Kyoto University, Kyoto 606-8502, Japan.

 

significant decrease with the application of external magnetic field [2], suggesting an alternative origin of the heavy quasi-particles caused by factors such as valence fluctuations [3]. An additional important issue that has been left unsolved is the contribution to the physical properties from the anharmonic vibrations of the filled R ion in the oversized cage (so-called 'rattler') [1]. It is also emerging that the physical properties are largely influenced by the extent of the R-filling rate.

The physical properties of skutterudites filled with heavy lanthanide elements are rather less studied, which has restricted systematic studies on the intriguing properties that stem from the peculiar crystal structure. This is mainly because of the difficulties of synthesizing compounds with good quality. Recently, some polycrystalline samples of new skutterudites $RFe_4X_{12}$ with sufficient filling of the heavy rare-earth atoms have been successfully synthesized by preparing them at high pressures and high temperatures [4]. In this paper, we focus on the HFL skutterudite $YbFe_4Sb_{12}$ and the related compound $LaFe_4Sb_{12}$.

$YbFe_4Sb_{12}$ provides a convenient laboratory to investigate the important issues described above, since it has: (1) non-integer valence between $Yb^{2+}$ and $Yb^{3+}$ [4], (2) a heavy fermion ground state ($\gamma \simeq 0.14$ J mol$^{-1}$ K$^{-2}$) [5], and (3) possible thermal vibrations of Yb ion in the Sb cage. The magnetic properties of the compounds with Yb-deficiency, $Yb_xFe_4Sb_{12}$ ($0.875 < x < 0.910$) synthesized at atmospheric pressure, are known to be largely modified by changing the Yb-filling rate $x$ [5–7]. Systematic studies of the magnetization and electron-probe microanalysis (EPMA) of the chemical constituent indicated that the single crystals with $x$ less than ∼0.91 exhibit a weak ferromagnetic (FM) order, and the ordering temperature $T_C$ increases with decreasing $x$ [8, 9]. It was suggested that the paramagnetic ground state would be realized for compounds with $x$ larger than ∼0.93.

For the related compound $LaFe_4Sb_{12}$ with no 4f electrons, the magnetic susceptibility at high temperature shows a Curie–Weiss (CW)-like behaviour [10, 11] which is characteristic of the localized electrons. The susceptibility at low temperatures shows a stronger temperature dependence than the CW behaviour and the value at 4.2 K is more than one order of magnitude larger than that in other La-based skutterudite compounds, whereas a large $\gamma$ of ≃0.19 J mol$^{-1}$ K$^{-2}$ of $La_{0.83}Fe_4Sb_{12}$ suggests a heavy fermion ground state [12, 13]. The nuclear magnetic resonance (NMR) measurements on $La_{0.88}Fe_4Sb_{12}$ suggested an HFL state at low temperatures below ∼5 K [15].

In order to provide important information to solve the issues that have been left unsolved from a microscopic point of view, we have carried out $^{121}$Sb nuclear quadrupole resonance (NQR) and $^{139}$La NMR studies by using almost completely filled (stoichiometric) materials of $YbFe_4Sb_{12}$ and $LaFe_4Sb_{12}$ synthesized at high pressures. The experimental details and results are reported in section 2. In sections 3.1 and 3.2, we discuss the electronic states of the stoichiometric skutterudites. The effect of rare-earth deficiency is also discussed by comparing the NQR and NMR data of the present study with those previously reported for the compounds synthesized at ambient pressure. The origin of the relaxation anomalies observed at low temperatures are discussed in section 3.3 in terms of possible thermal vibrations of R ions in the Sb cage. In section 4, we present some concluding remarks.

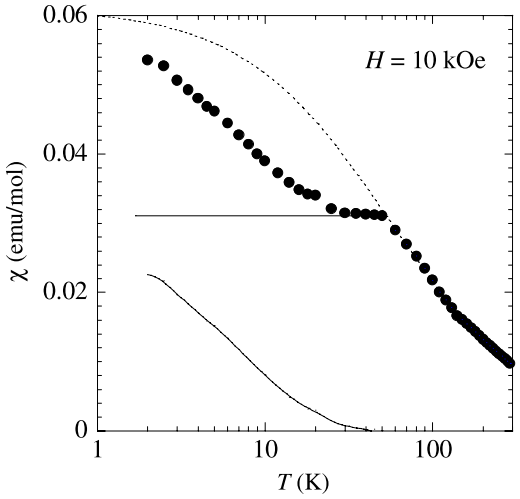


**Figure 1.** Temperature dependence of the magnetic susceptibility $\chi$ of $YbFe_4Sb_{12}$ synthesized at high pressure (cited from [4]). The broken curve is the best fit of the Curie–Weiss law with the data above 80 K. A solid line and a solid curve are the Pauli paramagnetic and Curie-tail terms, respectively, extracted from the experimental data below 50 K.

## 2. Experimental details and results

### *2.1. Magnetic susceptibility*

The temperature dependence of the magnetic susceptibility $\chi$ of $YbFe_4Sb_{12}$ compound used in the present study is shown in figure 1 (cited from [4]). $\chi$ at high temperatures above ∼80 K can be reproduced by the CW law with the effective magnetic moment $\mu_{\rm eff} \simeq 3.1\ \mu_B$ (Weiss temperature $\theta = -58$ K) smaller than 4.54 $\mu_B$ of the $Yb^{3+}$ ion. Upon cooling below ∼50 K, $\chi$ exhibits a saturation behaviour, suggesting that the compound transforms into an HFL ground state due to the coherent Kondo scattering [16]. At lower temperatures below ∼20 K, $\chi$ exhibits another CW-type increase, which could be ascribed to either the incomplete Yb-filling, or spurious magnetic impurity phases, or both. Indeed, the experimental $\chi$ data below ∼50 K can be decomposed into a temperature-independent term and a Curie-tail term as shown in the figure by a solid line and a solid curve, respectively.

### *2.2. $^{121}$Sb-NQR and $^{139}$La-NMR spectra*

The NQR measurement in zero field and NMR measurement in fields were carried out by using a wide-band phase-coherent pulsed NMR spectrometer in a temperature range between $T =$ 1.4 and 150 K. The NQR spectra of $YbFe_4Sb_{12}$ obtained by a frequency sweeping procedure consists of two resonance lines of $^{121}$Sb (nuclear spin $I = 5/2$, gyromagnetic ratio $\gamma_N/2\pi =$ 1.0189 kHz Oe$^{-1}$, electric quadrupole moment $Q = -0.53$ b) at frequencies near 44 and 76 MHz, and three resonance lines of $^{123}$Sb ($I = 7/2$, $\gamma_N/2\pi = 0.551\,75$ kHz Oe$^{-1}$,

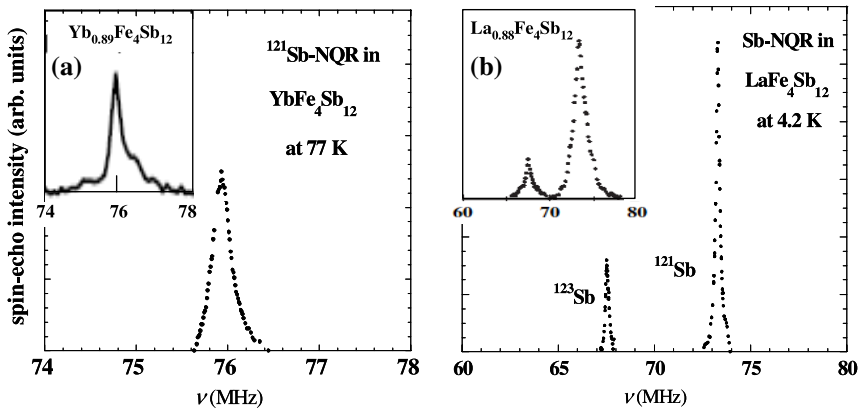


**Figure 2.** NQR spectrum of $^{121}$Sb in (a) $YbFe_4Sb_{12}$ at 77 K and (b) $LaFe_4Sb_{12}$ at 4.2 K. Insets show the $^{121}$Sb spectrum in the corresponding compounds with incomplete rare-earth filling (cited from [14] and [15]).

$Q = -0.68$ b) near 34, 44, and 73.4 MHz. Figure 2(a) shows the $^{121}$Sb-NQR line of $|\pm 3/2\rangle \leftrightarrow |\pm 5/2\rangle$ transition in $YbFe_4Sb_{12}$, and figure 2(b) the $^{121}$Sb-NQR lines of the $|\pm 3/2\rangle \leftrightarrow |\pm 5/2\rangle$ transition and $^{123}$Sb-NQR line of the $|\pm 5/2\rangle \leftrightarrow |\pm 7/2\rangle$ transition, respectively. The NQR lines previously reported for $Yb_{0.89}Fe_4Sb_{12}$ [14] and $La_{0.88}Fe_4Sb_{12}$ [15] are cited in the inset of each figure for comparison.

A single NMR line of $^{139}$La ($I = 7/2$, $\gamma_n/2\pi = 0.601\,46$ kHz Oe$^{-1}$) in $LaFe_4Sb_{12}$ was obtained by a field sweeping procedure at a fixed frequency 28.25 MHz. Figure 3 shows the resonance line observed at several fixed temperatures between 4.2 and 100 K. Here, each of the spectra at different temperatures was appropriately shifted along the vertical axis. On the other hand, the $^{139}$La-NMR spectrum in $La_{0.88}Fe_4Sb_{12}$ cited in the inset for comparison [15] has a somewhat complex structure.

As can be seen in figures 2 and 3, both the NQR and NMR lines of the compounds used in the present study have a Lorentzian-type shape with considerably smaller linewidth than that previously reported for the compounds with incomplete R-filling of about $x \sim 0.9$. The two satellite lines of $^{139}$La-NMR observed for $La_{0.88}Fe_4Sb_{12}$ (inset of figure 3) disappeared in the sample of the present study. These results indicate a good quality (sufficient R-filling) of samples synthesized at high pressures.

The frequencies of two $^{121}$Sb-NQR lines are well reproduced by numerically calculating the Hamiltonian of the quadrupole interaction between the nuclear electric quadrupole moment $Q$ and the electric field gradient (EFG) $q = V_{zz}$

$$\mathcal{H}_Q = \frac{e^2qQ}{4I(2I-1)}[(3I_z^2 - I^2) + \eta(I_x^2 - I_y^2)], \qquad (1)$$

with the quadrupole resonance frequency

$$\nu_Q = 3e^2qQ/2hI(2I-1) \qquad (2)$$

and asymmetry parameter $\eta = [V_{xx} - V_{yy}]/V_{zz}$ as fitting parameters. The extracted value $\eta = 0.373$ for $YbFe_4Sb_{12}$ is in good agreement with that previously reported for the single crystal of $Yb_{0.89}Fe_4Sb_{12}$ [14].

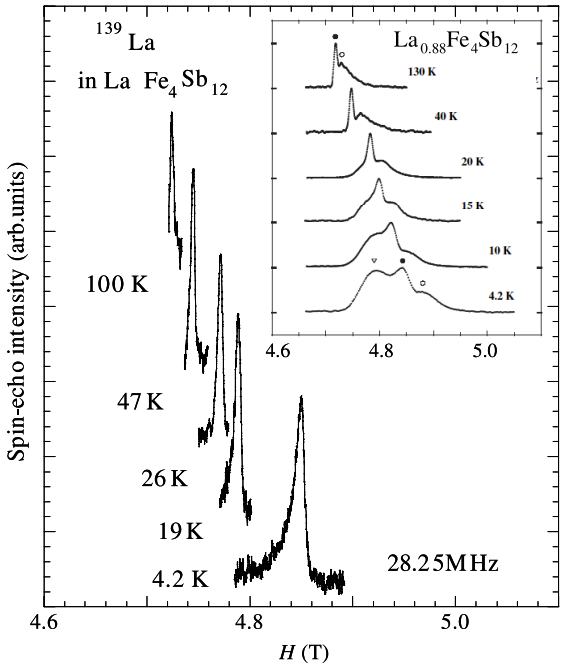


**Figure 3.** NMR spectra of $^{139}$La in $LaFe_4Sb_{12}$. Each of the spectra at different temperatures is appropriately shifted along the vertical axis. The inset shows the $^{139}$La NMR spectra in the compound with incomplete La filling (cited from [15]).

The full-width at half-maximum (FWHM) of the $^{121}$Sb-NQR line at $\simeq$76 MHz in $YbFe_4Sb_{12}$ is plotted in figure 4 against temperature on a semi-log scale. Upon cooling, the FWHM exhibits a large stepped increase near 30 K and a small increase near 4 K. This result contrasts with the markedly large linewidth broadening below the FM transition temperature ($T_C \simeq 18$ K) observed for the compound with Yb-deficiency ($x = 0.89$) [14]. Shown in figure 5 is the temperature dependence of $\nu_Q$ deduced from the spectrum analysis of $^{121}$Sb-NQR lines. Upon cooling, $\nu_Q$ initially exhibits a monotonic increase down to $\sim$50 K, which can be ascribed to the shrinking of the unit-cell volume. Below $\sim$50 K, $\nu_Q$ is independent of temperature.

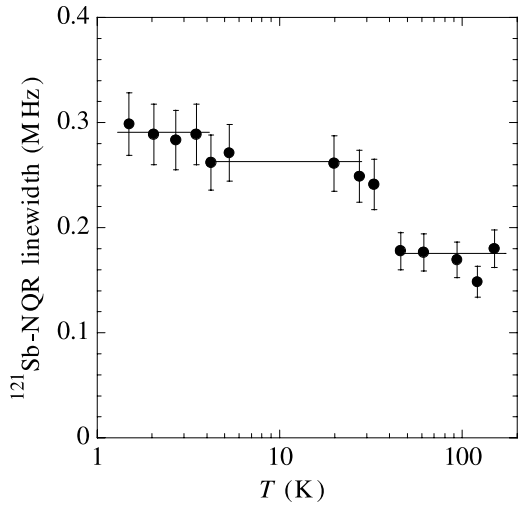


**Figure 4.** Temperature dependence of the full-width at half-maximum (FWHM) of the $^{121}$Sb-NQR line at $\simeq$76 MHz in $YbFe_4Sb_{12}$.

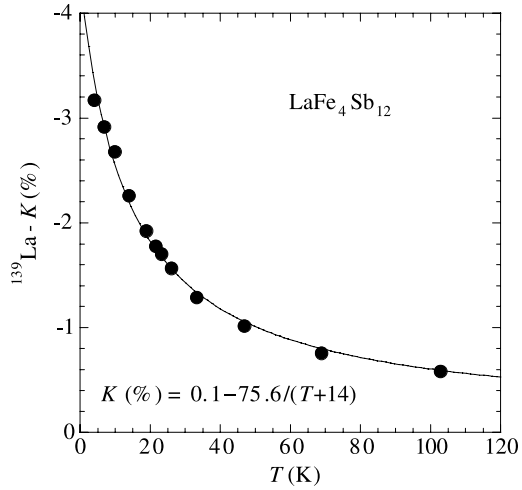


**Figure 6.** Temperature dependence of the Knight shift $K$ of $^{139}$La in $LaFe_4Sb_{12}$. Solid curve is the best fit of the Curie–Weiss law with the data.

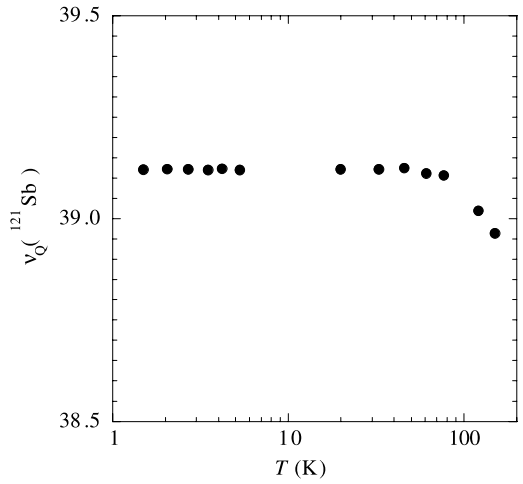


**Figure 5.** Temperature dependence of the $^{121}$Sb nuclear quadrupole frequency $\nu_Q$ in $YbFe_4Sb_{12}$.

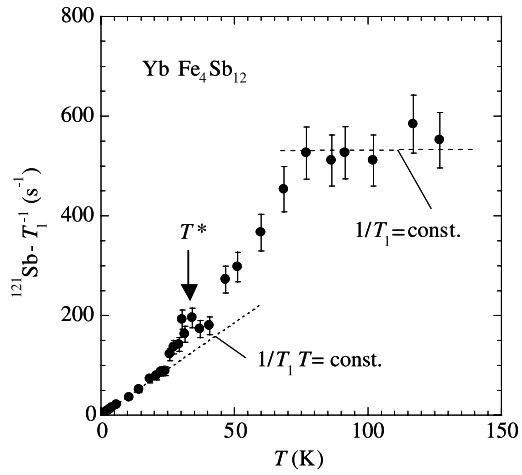


**Figure 7.** Nuclear spin–lattice relaxation rate $1/T_1$ of $^{121}$Sb in $YbFe_4Sb_{12}$ in zero field plotted against temperature. The broken lines drawn in the figure are guides for the eye.

The Knight shift $K = (H_0 - H_{res})/H_{res}$ of $^{139}$La in $LaFe_4Sb_{12}$ was determined from the resonance field $H_{res}$ at the peak intensity point of the NMR line. Here, $H_0 = 2\pi\nu_N/\gamma_N$ is the resonance field of an isolated nucleus. $K$ is given by the local magnetic field on a given nucleus, and is proportional to the uniform magnetic susceptibility $\chi(q = 0)$. Upon cooling, the value of $^{139}$La–K in $LaFe_4Sb_{12}$ exhibits a CW-type increase down to $T = 1.4$ K, as plotted in figure 6 against temperature. Thus, the stronger temperature dependence of $\chi$ at lower temperatures than the CW behaviour expected from the high-temperature data [10, 11] is reasonably ascribed to a small amount of spurious magnetic impurities.

### *2.3. Nuclear spin–lattice relaxation rate*

The longitudinal nuclear spin–lattice relaxation rate $1/T_1$ divided by $T$ reveals the spin fluctuation properties from the wavevector $q$-averaged dynamical spin susceptibility $\chi(q)$ at frequencies in the vicinity of $\nu_N$.

The evolution of low-energy spin fluctuations in $YbFe_4Sb_{12}$ was investigated through the $1/T_1$ measurement at the peak intensity point of the $^{121}$Sb-NQR line near 76.0 MHz (figure 2(a)). The nuclear magnetization recovery $M(t)$ at time $t$ after the initial single rf saturation pulse shows multi-exponential behaviour, and it can be satisfactorily reproduced by the relation [17]

$$[M(\infty) - M(t)]/M(\infty) = a\mathrm{e}^{-3t/T_1} + (1-a)\mathrm{e}^{-10t/T_1}. \quad (3)$$

The extracted values of $T_1$ are plotted in figure 7 against temperature. $1/T_1$ at high temperatures above $\sim$80 K exhibits near $T$-independent behaviour, $1/T_1T$ ($\propto \Sigma_q \chi(q)$) follows the CW law. This result indicates that $1/T_1$ at high temperatures is dominated by the relaxation process to the spin fluctuations of localized 4f electrons [18]. Below $\sim$20 K, $1/T_1$ is nearly proportional to temperature, which is characteristic of the Fermi liquid state.

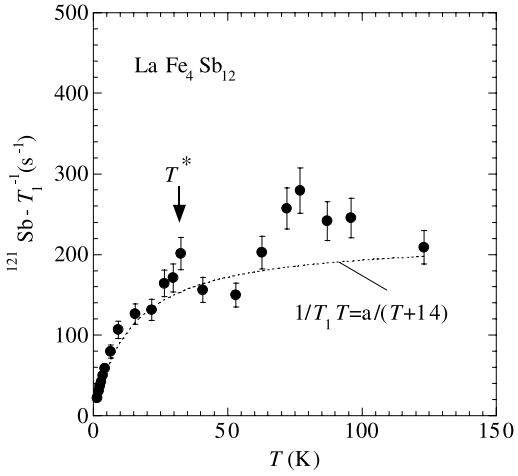


**Figure 8.** Nuclear spin–lattice relaxation rate $1/T_1$ of $^{121}$Sb in $LaFe_4Sb_{12}$ in zero field plotted against temperature. The broken curve is the best fit of the Curie–Weiss law with the data.

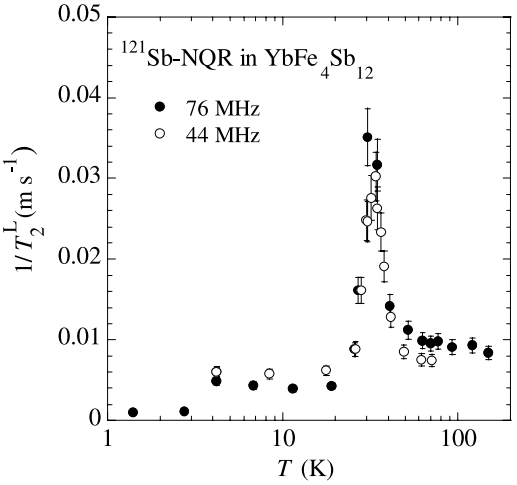


**Figure 10.** $^{121}$Sb-$1/T_2$ in $YbFe_4Sb_{12}$ plotted against temperature on a semi-log scale.

Shown in figure 8 is the temperature dependence of $^{121}$Sb-$1/T_1$ in $LaFe_4Sb_{12}$ measured at the peak intensity point of the NQR line near 73.4 MHz (figure 2(b)). The $1/T_1$ data can be roughly reproduced by the Curie–Weiss law with the Weiss temperature $\theta = -14$ K, as is shown in the figure by the broken curve.

### *2.4. Nuclear spin–spin relaxation rate*

The transversal nuclear spin–spin relaxation rate $1/T_2$ in solids is basically dominated by the spin flip-flop term $I_i^+ I_j^-$ of dipolar interactions between neighbouring nuclei. The temperature-independent $1/T_2$ is proportional to the inverse of the NMR linewidth. The low-frequency fluctuations in the energy splitting of nuclear spin levels induce an additional transversal relaxation, which originates from the local magnetic field fluctuations associated with either the spin fluctuations of neighbouring electrons or the motion of atoms, or both.

$T_2$ of $^{121}$Sb in $YbFe_4Sb_{12}$ was measured at the peak intensity point of the NQR line near 76 and 44 MHz by measuring the spin-echo intensity $M(2\tau)$ as a function of time separation $\tau$ between $\pi/2$ and $\pi$ rf pulses. The $M(2\tau)$ data can be reproduced by the single exponential (Lorentzian) decay curve

$$M(2\tau) = M(0)\mathrm{e}^{-2\tau/T_2^{\mathrm{L}}}, \tag{4}$$

in the whole temperature range of the present measurement (figure 9(a)). The values of $1/T_2^{\mathrm{L}}$ data are plotted in figure 10 against temperature on a semi-log scale. The subsequent stepped decreases of $1/T_2^{\mathrm{L}}$ below ∼20 and ∼4 K correspond to the two stepped NQR linewidth broadenings shown in figure 4. A marked feature in figure 10 is the large sharp $1/T_2^{\mathrm{L}}$ peak at temperatures in the vicinity of $T^* \simeq 32$ K. The fit of the decay curve (equation (4)) with the $M(2\tau)$ decay data at temperatures close to $T^*$ was rather poor, because the spin-echo intensity rapidly decreases and the signal almost disappears due to the extremely large $1/T_2^{\mathrm{L}}$.

$T_2$ in $LaFe_4Sb_{12}$ was measured by using both $^{121}$Sb-NQR and $^{139}$La-NMR lines. The spin-echo intensity $M(2\tau)$ of $^{121}$Sb exhibits Lorentzian decay, and a partial Gaussian decay component emerges only in the vicinity of $T^*$, as shown in

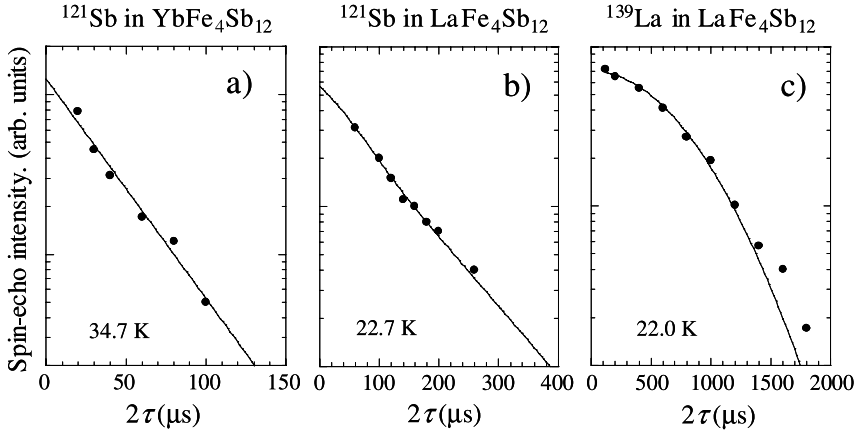


**Figure 9.** Spin-echo intensity $M(2\tau)$ plotted against time separation $\tau$ between $\pi/2$ and $\pi$ rf pulses at temperatures close to the $1/T_2$ maximum: (a) $^{121}$Sb in $YbFe_4Sb_{12}$, (b) $^{121}$Sb in $LaFe_4Sb_{12}$, (c) $^{139}$La in $LaFe_4Sb_{12}$. The solid line in each figure is the best fit of $M_0^{\mathrm{L}} \exp[-2\tau/T_2^{\mathrm{L}}]$, $M_0^{\mathrm{G}} \exp[-(2\tau)^2/T_2^{\mathrm{G}}] + M_0^{\mathrm{L}} \exp[-2\tau/T_2^{\mathrm{L}}]$, and $M_0^{\mathrm{G}} \exp[-(2\tau)^2/T_2^{\mathrm{G}}]$ with the data.

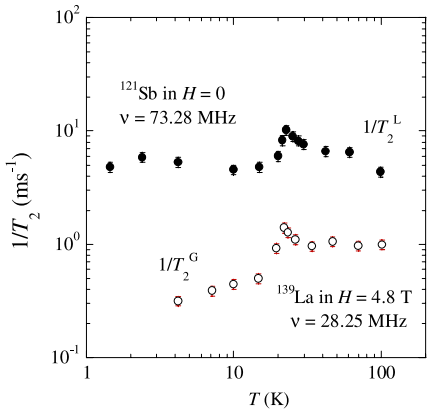


**Figure 11.** $1/T_2$ of $^{121}$Sb and $^{139}$La in $LaFe_4Sb_{12}$ measured by using $^{121}$Sb-NQR in zero field (filled circles) and $^{139}$La-NMR in a field of 4.8 kOe (open circles).

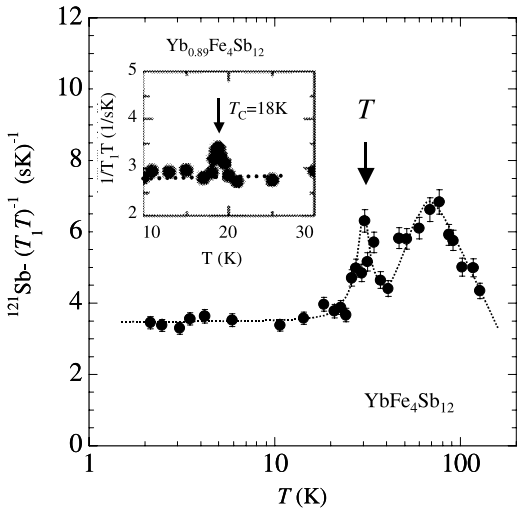


**Figure 12.** $1/T_1T$ of $^{121}$Sb in $YbFe_4Sb_{12}$ in zero field plotted against temperature. The broken line drawn in the figure is a guide for the eye. The inset shows the $1/T_1T$ data for the compound with incomplete Yb-filling cited from [14].

figure 9(b). In contrast, $M(2\tau)$ of $^{139}$La exhibits Gaussian decay

$$M(2\tau) = \mathrm{e}^{-(2\tau)^2/T_2^{G}}, \tag{5}$$

within the whole temperature range of present measurements (figure 9(c)). As shown in figure 11, each of $^{121}$Sb-$1/T_2^{L}$ and $^{139}$La-$1/T_2^{G}$ exhibits the local maximum at $T^* \simeq 23$ K.

## 3. Discussion

### *3.1. Electronic state of $YbFe_4Sb_{12}$*

It has been unclear whether the magnetism of $YbFe_4Sb_{12}$ originates from the 4f electrons of the Yb ion or the 3d electrons of Fe in the $[Fe_4P_{12}]$ anion, or both. At first we discuss the electronic state of the compound synthesized at high pressures. The Lorentzian-type shape of the $^{121}$Sb-NQR line with small linewidth and the absence of FM ordering down to 1.4 K indicate that the extent $x$ of Yb-filling is close to unity. The CW-type susceptibility $\chi$ at high temperatures above ∼80 K is indicative of the localized 4f electron state. The temperature-independent $1/T_1$ at high temperatures (figure 7) provides microscopic evidence for the localized 4f electron state.

Remarkable features can be seen in the $1/T_1T$ versus $T$ plots shown in figure 12. Upon cooling, $1/T_1T$ begins to deviate from the initial CW-type increase, takes the broad maximum around 80 K, and turns to a rapid decrease followed by a $1/T_1T$ plateau at low temperatures below ∼10 K. The origin of the local $1/T_1T$ maximum can generally be ascribed to either the coherent Kondo interaction or the crossover valence transition, or both. For the Kondo interaction, the numerical calculation of the $J = 7/2$ Coqblin–Schrieffer model predicts a local maximum in the uniform susceptibility $\chi(q = 0)$ [19]. However, the experimental $\chi$ shown in figure 1 does not display any corresponding anomaly. The crossover valence transition is evidenced by observing the expansion of the unit-cell volume $v_c$. But, as shown in figure 5, the NQR frequency $\nu_Q$ which is inversely proportional to $v_c$ displays a monotonic increase with decreasing temperature down to ∼50 K followed by saturation behaviour. Thus, at present, it is not easy to clarify definitely the cause of the anomalous low-energy spin fluctuation behaviour observed at temperatures near 80 K, and further experimental and theoretical studies are needed to shed light on it.

The $1/T_1T$ plateau at lower temperatures below ∼20 K provides microscopic evidence that $YbFe_4Sb_{12}$ has a nonmagnetic heavy fermion ground state, and the constant value of $1/T_1T$ is proportional to the square of the density of states $N(E_F)$ at the Fermi level $E_F$. On the other hand, the single crystals of $Yb_xFe_4Sb_{12}$ ($0.875 < x < 0.910$) with the CW-type $\chi$ ($\mu_{eff} \simeq 2.9\ \mu_B$, $\theta \simeq 53$–$70$ K) at high temperatures exhibit weak FM order [9]. With decreasing $x$ from 0.910 to 0.875, the FM ordering temperature $T_C$ increases from 5 to 17 K, and the very small saturation moment $\mu_0$ increases from 0.005 to 0.066 $\mu_B$/f.u. Based on the fact that the alkali-metal skutterudites $NaFe_4Sb_{12}$ and $KFe_4Sb_{12}$ are weak itinerant ferromagnets with $\mu_0 \simeq 0.25\ \mu_B$/Fe(f.u.) below $T_C \simeq 85$ K [20, 21]. Ikeno *et al* conjectured that the magnetic moment solely originates from the itinerant 3d electrons of Fe in the anion $[Fe_4Sb_{12}]$, and the Yb ion is thought to be stably divalent [9].

A key to solving the antagonistic conclusions of the dominant 4f electron contribution for $YbFe_4Sb_{12}$ and the 3d one for $Yb_xFe_4Sb_{12}$ ($0.875 < x < 0.910$) can be found by comparing the $1/T_1T$ data for each compound. The inset of figure 12 shows the $1/T_1T$ data for $Yb_{0.89}Fe_4Sb_{12}$ at low temperatures reported by Kawaguchi *et al* (cited from [14]). They focused on the $1/T_1T$ cusp at ≃18 K accompanied by the extremely large NQR linewidth broadening, and ascribed it to the FM ordering that originates from the itinerant 3d electrons of Fe in the $[Fe_4Sb_{12}]$ anion [14]. However, it is worth noting that the low-temperature $1/T_1T$ data display the $1/T_1T$ = constant behaviour as a whole. The values of $1/T_1T \simeq 3.4$ (s K)$^{-1}$ for $YbFe_4Sb_{12}$ and ≃2.9 (s K)$^{-1}$ for $Yb_{0.89}Fe_4Sb_{12}$ indicate that the introduction of Yb-deficiency ($x = 0.89$)

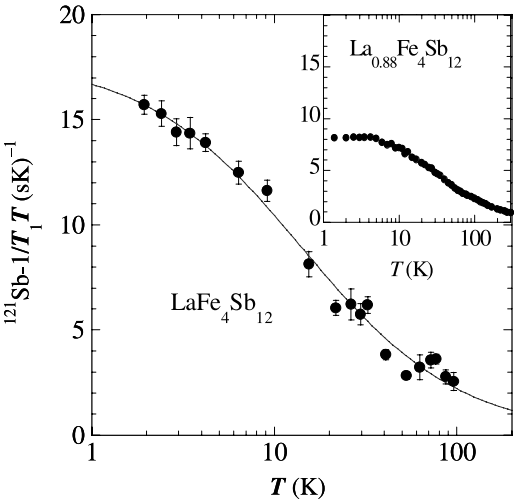


**Figure 13.** $1/T_1T$ of $^{121}$Sb in $LaFe_4Sb_{12}$ in zero field plotted against temperature. The solid curve is the best fit of the Curie–Weiss law with the data. The inset shows the $1/T_1T$ data for the compound with incomplete La filling, cited from [15].

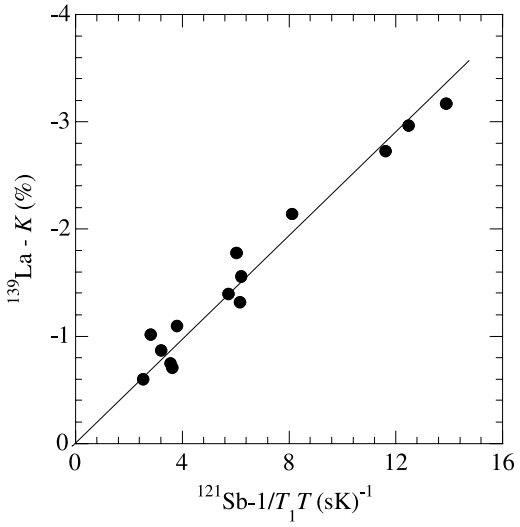


**Figure 14.** $^{139}$La Knight shift plotted against $^{121}$Sb-$1/T_1T$ in $LaFe_4Sb_{12}$ with temperature being an implicit parameter.

reduces $N(E_F)$ by about 8.6%. Thus, we may conclude that in $Yb_xFe_4Sb_{12}$ with a small amount of Yb-deficiency, the 4f electrons play the dominant role on the formation of heavy fermions, and the 3d electrons of Fe play the concomitant role on the weak FM order.

The band structure calculation for $YbFe_4Sb_{12}$ found by using a full-potential linear augmented plane-wave (FLAPW) method by Takigahara *et al* [22] indicates that both the Yb 4f bands and Fe 3d bands are located just below $E_F$ and partially cross the Fermi sea. However, present NQR studies indicate that the tail of the 3d density of states (DOS) in the stoichiometric material ($x = 1$) hardly crosses $E_F$. The appearance of FM order with decreasing $x$ suggests that the introduction of Yb-deficiency causes an equivalent effect with hole doping to push down the Fermi level, yielding the concomitant contribution of the 3d bands.

### 3.2. Electronic state of $LaFe_4Sb_{12}$

The values $^{121}$Sb-$1/T_1T$ in $LaFe_4Sb_{12}$ were plotted in figure 13 against temperature on a semi-log scale, and those in $La_{0.88}Fe_4Sb_{12}$ cited from [15] were shown in the inset. Upon cooling $LaFe_4Sb_{12}$ down to $T = 1.4$ K, $1/T_1T$ exhibits a CW-type increase. The $^{139}$La-$K$ versus $^{121}$Sb-$1/T_1T$ plots shown in figure 14 are on a straight line, indicating that $1/T_1T$ is dominated by the uniform susceptibility $\chi(q = 0)$. This result provides microscopic evidence that $LaFe_4Sb_{12}$ remains in the spin paramagnetic state at low temperatures, at least down 1.4 K, and it originates most probably from the 3d electrons of Fe in the $[Fe_4Sb_{12}]$ anion. This conclusion is incompatible with the heavy fermion ground state of $La_{0.83}Fe_4Sb_{12}$ inferred from the large $\gamma$ of $\simeq$0.19 J mol$^{-1}$ K$^{-2}$ [12, 13] and that of $La_{0.88}Fe_4Sb_{12}$ suggested by the $1/T_1T$ plateau below $\sim$5 K (inset of figure 13 [15]). However, it is unacceptable that the introduction of a small amount of La deficiency changes the ground state from the spin paramagnetic to a heavy Fermion state. Indeed $K$ of $^{139}$La in $La_{0.88}Fe_4Sb_{12}$ follows the CW law down to 1.4 K [15]. The plateau-like behaviour of $1/T_1T$ in $La_{0.88}Fe_4Sb_{12}$ may be caused by the experimental uncertainty in extracting the intrinsic $1/T_1$ values from the nuclear magnetization recovery $M(t)$ observed by using the complex $^{139}$La NMR spectrum shown in the inset of figure 3.

### 3.3. Vibrations of Sb cages and/or R ion filled in the cage

In this subsection, we discuss the origin of the $1/T_2$ peaks observed in both $YbFe_4Sb_{12}$ and $LaFe_4Sb_{12}$. Similar $1/T_2$ peaks have not been reported for the filled skutterudites with P cages, but some of the skutterudites with Sb cages, i.e. $PrOs_4Sb_{12}$ at $T^* \simeq 25$ K and $T^{*\prime}\simeq$150 K, $SmOs_4Sb_{12}$ at $T^* \simeq 20$ K and $T^{*\prime}\simeq$120 K [23]. The oversized Sb cage is considered to allow thermal vibrations of the cages and/or the R ion filled in each cage. Among the thermal vibrations, a possible R ion motion between off-centre equivalent positions within the cage is a so-called 'rattler'. Raman scattering measurements by Ogita *et al* observed second-order phonons, including the vibration of R ions with a flat phonon dispersion in the spectra of $SmRu_4Sb_{12}$ and $ROs_4Sb_{12}$ [24]. Thus, the origin of $1/T_2$ anomalies at $T^*$ and $T^{*\prime}$ has been discussed in terms of the rattling of the R ion and the pnictogen vibrations, respectively [25].

As shown in figure 10, $YbFe_4Sb_{12}$ of the present study displays a large $1/T_2$ peak at $T^* \simeq 32$ K, although the second-order phonon is hardly observed in the Raman scattering spectrum of $Yb_xFe_4Sb_{12}$ [24]. If a crystal structure phase transition took place, $1/T_2$ and $\nu_Q$ would display a stepped change at temperatures in the vicinity of $T^*$, and this is not the present case. These features lead to a conjecture that the thermal vibrations of either the Sb cages or Yb ion in each Sb cage, or both, freeze at temperatures near $T^*$. Upon cooling close to $T^*$, frequencies of the thermal vibrations rapidly decrease and cross over $\sim 1/2\tau$, which is able to yield the experimental $1/T_2$ peak. It is worth noting that

$LaFe_4Sb_{12}$ with no f electron also displays the $1/T_2$ peak at $T^* = 23$ K, as shown in figure 11. This result indicates that the spin fluctuations of the Yb 4f electron are not a necessary condition for the relaxation anomalies, and supports the conclusion that the phonon instability originating from the peculiar crystal structure of skutterudites plays a primary role. The $1/T_2$ peak of $YbFe_4Sb_{12}$ is much larger than that of $LaFe_4Sb_{12}$. The enhancement of the $1/T_2$ peak in $YbFe_4Sb_{12}$ could be explained by the additional markedly large fluctuating magnetic field on the given nuclei, originating from the 4f electron spin on the vibrating Yb ion within the Sb cage.

The phonon instabilities with frequencies close to $\nu_N$ would also contribute to the longitudinal spin–lattice relaxation, in addition to the dominant spin and/or conduction relaxations. We firstly succeeded in observing a small $1/T_1$ peak at $T^* = 32$ K for $YbFe_4Sb_{12}$ and at 33 K for $LaFe_4Sb_{12}$, although the data are largely scattered due to the poor NQR intensity in the vicinity of $T^*$. The $1/T_2$ and $1/T_1$ peaks at the same temperature for the $YbFe_4Sb_{12}$ case indicate that the thermal vibrations of Sb cages or Yb ions in the cage are quenched very rapidly in a small temperature range, suggesting a correlated thermal motion caused by possible interactions between f electrons in neighbouring Sb cages. Neither the $1/T_1$ peak nor the disappearance (nor significant decrease) of the NQR signal was reported for $Yb_{0.89}Fe_4Sb_{12}$ [14]. Thus, the disorder introduced by incomplete Yb-filling is considered to disturb the correlated motion, making it difficult to observe the $1/T_2$ (and $1/T_1$) peak.

## 4. Conclusion

We have carried out an NQR study of $^{121}$Sb in the filled skutterudite $YbFe_4Sb_{12}$ synthesized at high pressure, in order to elucidate the low-energy spin fluctuation phenomena. $^{121}$Sb-NQR and $^{139}$La-NMR measurements on the related compound $LaFe_4Sb_{12}$ with no 4f electron have also been carried out for comparison. The $1/T_1$ measurement of $^{121}$Sb in $YbFe_4Sb_{12}$ provides evidence that upon cooling below ∼20 K, the compound transforms from the localized 4f electron state of $Yb^{3+}$ ions to a nonmagnetic heavy Fermi liquid state, which originates from the mixing of 4f electrons with conduction electrons, whereas the CW-type behaviour of the $^{139}$La Knight shift and $^{121}$Sb-$1/T_1$ in $LaFe_4Sb_{12}$ indicate that the compound remains in the localized electron state down to 1.4 K, and it originates from 3d electrons of Fe in $[Fe_4Sb_{12}]$ anions. In both compounds, $1/T_2$ exhibits a clear peak at $T^* \simeq 32$ and $\simeq$23 K, respectively. The origin of the $1/T_2$ peak is discussed in terms of the freezing of the thermal vibration of Sb cages or rare-earth ions filled in each Sb cage. By comparing the experimental results of the present study with those previously reported for the compounds synthesized at ambient pressure, it is pointed out that both the strongly correlated electron properties and the thermal vibrations are greatly modified with the increase of rare-earth atom deficiency.

## Acknowledgments

This work was partially supported by a Grant-in-Aid for Scientific Research from the Ministry of Education, Science and Culture of Japan, Grant No. 16340105, and also by a Grant-in-Aid for Scientific Research Priority Area, Skutterudite (Nos 15072202 and 18027002). One of the authors (AY) has been supported by the Japan Society for the Promotion of Science for Young Scientists.

## References

[1] Recent developments can be seen in many papers in Harima H, Kawamura H, Kitaoka Y, Kohno H, Miyake K, Suzuki Y, Sakakima H and Zheng G-q (ed) 2007 *Proc. 17th Int. Conf. on Magnetism*; *J. Magn. Magn. Mater.* 310
[2] Sanada S, Aoki Y, Aoki H, Tsuchiya A, Kikuchi D, Sugawara H and Sato H 2005 *J. Phys. Soc. Japan* **74** 246
[3] Ikeda H and Miyake K 1997 *J. Phys. Soc. Japan* **66** 3714
[4] Shirotani I, Araseki N, Shimaya Y, Nakata R, Kihou K, Sekine C and Yagi T 2005 *J. Phys.: Condens. Matter* **17** 4383
[5] Dilley N R, Freeman E J, Bauer E D and Maple M B 1998 *Phys. Rev.* B **58** 6287
[6] Leithe-Jasper A, Kaczorowski D, Rogl P, Bogner J, Reissner M, Steiner W, Wiesinger G and Godart C 1999 *J. Solid State Chem.* **109** 395
[7] Bauer E, Galatanu A, Michor H, Hilscher, Rogl G P, Boulet J and Noël H 2000 *Eur. Phys. J.* **14** 483
[8] Tamura I, Ikeno T, Mizushima T and Isikawa Y 2006 *J. Phys. Soc. Japan* **75** 014707
[9] Ikeno T, Mitsuda A, Kuwai T, Mizushima T, Isikawa Y and Tamura I 2008 *J. Magn. Magn. Mater.* at press
[10] Ravot D, Lafont U, Chapon L, Tedenac J C and Mauger A 2001 *J. Alloys Compounds* **323/324** 389
[11] Viennois R, Ravot D, Terki F, Hernandez C, Charar S, Haen P, Paschen S and Steglich S 2004 *J. Magn. Magn. Mater.* **272–276** e113
[12] Bauer E *et al* 2001 *Phys. Rev.* B **63** 224414
[13] Viennois R, Terki F, Errebbahi A, Charar S, Averous M, Ravot D, Tedenac J C, Haen P and Sekine C 2003 *Acta Phys.* B **34** 1221
[14] Kawaguchi M, Tou H, Sera M, Kojima K, Ikeno T and Isikawa Y 2006 *J. Phys. Soc. Japan* **75** 093702
[15] Magishi K, Nakai Y, Ishida K, Sugawara H, Mori I, Saito T and Koyama K 2006 *J. Phys. Soc. Japan* **75** 023701
[16] For example, Sumiyama A, Oda Y, Nagano H, Onuki Y, Shibutani K and Komatsubara T 1986 *J. Phys. Soc. Japan* **55** 1294
[17] Maclaughlin D E, Williamson J D and Butterworth J 1971 *Phys. Rev.* B **4** 60
[18] Moriya T 1956 *Prog. Theor. Phys.* **16** 614
[19] Sarrao J L *et al* 1999 *Phys. Rev.* B **59** 6855 and references therein
[20] Leithe-Jasper A, Schnelle W, Rosner H, Senthilkumaran N, Rabis A, Baenitz M, Gippius A, Morozova E, Mydosh J A and Grin Y 2003 *Phys. Rev. Lett.* **91** 037208
Leithe-Jasper A, Schnelle W, Rosner H, Senthilkumaran N, Rabis A, Baenitz M, Gippius A, Morozova E, Mydosh J A and Grin Y 2003 *Phys. Rev. Lett.* 2004 **93** 089904
[21] Leithe-Jasper A *et al* 2004 *Phys. Rev.* B **70** 214418
[22] Takegahara K and Harima H 2002 *J. Phys. Soc. Japan* **71** 240–2
[23] Kotegawa H, Hidaka H, Shimaoka Y, Miki T, Kobayashi T C, Kikuchi D, Sugawara H and Sato H 2005 *J. Phys. Soc. Japan* **74** 2173
[24] Ogita N *et al* 2007 *J. Magn. Magn. Mater.* **310** 948
[25] Kotegawa H, Yogi M, Imamura Y, Kawasaki Y, Zheng G.-Q, Kitaoka Y, Ohsaki S, Sugawara H, Aoki Y and Sato H 2003 *Phys. Rev. Lett.* **90** 027001 and private communications